In vitro evaluation of free-form biodegradable bone plates for fixation of distal femoral physeal fractures in dogs

Denis J. Marcellin-Little, DEDV; Brian J. Sutherland, DVM; Ola L. A. Harrysson, PhD; Erica S. Lee, MS

Objective—To design and manufacture free-form biodegradable polycaprolactone (PCL) bone plates and to compare mechanical properties of femoral constructs with a distal physeal fracture repaired by use of 5 stabilization methods.

Sample Population—40 canine femoral replicas created by use of additive manufacturing and rapid tooling.

Procedures—Surgery duration, mediolateral and craniocaudal bending stiffness, and torsional stiffness of femoral physeal fracture repair constructs made by use of 5 stabilization methods were assessed. The implants included 2 Kirschner wires inserted medially and 2 inserted laterally (4KW), a commercial stainless steel plate (CSP), a custom free-form titanium plate (CTP), thin (2-mm-thick) biodegradable PCL plates (TNP) placed medially and laterally, and thick (4-mm-thick) PCL plates (TKP) placed medially and laterally.

Results—Surgical placement of 4KW was more rapid than placement of other implants. The mean caudal cantilever bending stiffness of CTP and CSP constructs was greater than that for TNP, TKP, and 4KW constructs, and the mean caudal cantilever bending stiffness of TNP and TKP constructs was greater than that for 4KW constructs. The mean lateral cantilever bending stiffness of TKP constructs was greater than that for 4KW constructs. Differences among construct types were not significant in yield strength, ultimate strength, yield torque, and ultimate torque.

Conclusions and Clinical Relevance—The mechanical properties of fracture repair constructs made from free-form PCL biodegradable plates compared favorably with those of constructs made from Kirschner wires. The impact of PCL plates on musculoskeletal soft tissues, bone healing, and bone growth should be evaluated before clinical use. (*Am J Vet Res* 2010;71:1508–1515)

Physeal fractures in dogs are commonly stabilized through the use of diverging Kirschner wires[1] but are rarely managed with bone plates because of the short length of epiphyseal fragments and because bone plates limit longitudinal bone growth.[2] The presence of Kirschner wires (Rush pins) may also limit longitudinal bone growth.[3] Biodegradable, polymer-based bone plates are sporadically used in orthopedics and are most often used to stabilize fragments of non–weight bearing bones (eg, skull fragments) after fractures and osteotomies.[4,5] Such bone plates were used successfully to stabilize radial fractures in 10 toy-breed dogs.[6] Free-form orthopedic implants are implants designed for specific applications. Fracture repairs made with free-form implants may be more stable than repairs made with conventional commercial implants because free-form implants can be better contoured to the bone surface than commercial implants.[7]

The purpose of the study reported here was to develop free-form biodegradable bone plates and assess the mechanical properties of constructs made with these plates. We hypothesized that constructs made from free-form biodegradable plates would have mechanical properties superior to constructs made from Kirschner wires but inferior to constructs

Abbreviations

4KW	Four Kirschner wires
CAD	Computer-aided design
CSP	Commercial stainless steel plate
CT	Computed tomography
CTP	Custom free-form titanium plate
Nm	Newton meter
PCL	Polycaprolactone
TKP	Thick polycaprolactone biodegradable plate
TNP	Thin polycaprolactone biodegradable plate

Received October 1, 2009.
Accepted November 24, 2009.
From the Department of Clinical Sciences, College of Veterinary Medicine (Marcellin-Little, Sutherland), Edward P. Fitts Department of Industrial and Systems Engineering (Harrysson), and Department of Biomedical Engineering (Lee), College of Engineering, North Carolina State University, Raleigh, NC 27606. Ms. Lee's present address is US Patent and Trademark Office, 600 Dulany St, Alexandria, VA 22314.
Supported by the University of North Carolina/NCSU Joint Department of Biomedical Engineering.
Address correspondence to Dr. Marcellin-Little (denis_marcellin@ncsu.edu).

made from metal bone plates. To test these hypotheses, we designed bone models of a physeal fracture in the distal portion of the canine femur and stabilized them by use of thin or thick biodegradable bone plates, custom or commercial metal bone plates, or Kirschner wires.

Materials and Methods

Bone models—A helical CT scan of the femur of a 5-month-old female Labrador Retriever was obtained with a 512 × 512 resolution and a 0° gantry tilt.[a] The CT scan was retro-reconstructed into 1-mm slices with a pixel size of 0.48 × 0.48 mm. The CT image was converted by use of a software program into four 3-D computer models of the cortex and cancellous bone that were optimized by means of the software's contrast, threshold, and region growing features.[b] The computer models of the cortical bone were exported as STL files, imported into modeling software,[c] and then smoothed with a haptic feedback device.[d] The files were subsequently imported into the CAD software.[e]

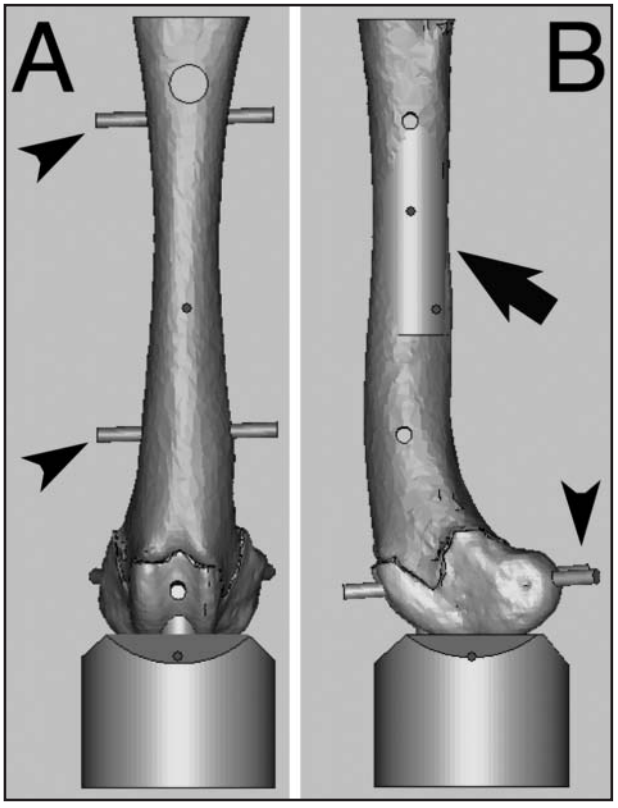

Figure 1—Illustration of the cranial (A) and medial (B) aspects of a 3-D rendering of a model built from a CT scan of a skeletally immature canine femur. Pegs were added to the cortical and cancellous regions of the proximal and distal portions of the model (arrowheads) to ensure proper alignment of the cancellous and cortical regions during casting. A cylinder was added to the rendering (arrow) to ensure proper alignment of the features. A 9.8-mm-diameter hole perpendicular to the long axis of the cylinder was placed at the proximal aspect of the model. A 50.8-mm-diameter cylinder parallel to the long axis of the cylinder was placed on the distal aspect of the model. Its sides were beveled to avoid interference with implants placed during surgery. The hole and cylinder were added to the proximal and distal portions of the model to ensure consistent placement on the materials testing machine.

A 50.8-mm-diameter cylinder parallel to the long axis of the bone was added to the distal portion of the bone, and a 9.8-mm-diameter hole perpendicular to the long axis of the bone was added to the proximal portion of the bone for connection to the materials testing machine (**Figure 1**). Replicas of the medullary and cortical bone for the proximal and distal portions of the bone were built in acrylonitrile butadiene styrene plastic by use of a fused deposition modeling free-form fabrication system.[f] These plastic replicas were used to make room-temperature (approx 32°C) vulcanized silicone rubber molds.[g] The medullary bones were cast by use of rigid polyurethane foam with a 1:1 ratio and were allowed to set for 24 hours.[h] The foam inserts were placed in the cortical bone molds, and cortical bones were cast by mixing bone powder[i] (30% by weight) and epoxy resin.[j] The models cured for > 24 hours. Then, the surface of the proximal femoral fragment models was coated with a thin layer of overlapping glass fibers sandwiched between 2 layers of epoxy resin.[j] Forty-five models of the proximal and distal portions of the femur, corresponding to a bone with a Salter-Harris type I fracture, were made. Five were used for preliminary testing.

Free-form biodegradable plate design and fabrication—The computer models of the cortical bone of the proximal and distal portions of the femur were merged by use of the CAD software.[e] Two- and 4-mm-thick plates were extruded from the medial and lateral bone surfaces. The plates were smoothed with the haptic feedback device software.[c] Six bevelled holes were added by use of the subtract function of the CAD software (**Figure 2**). The rapid tooling module of the CAD software was used to create free-form fabrication injec-

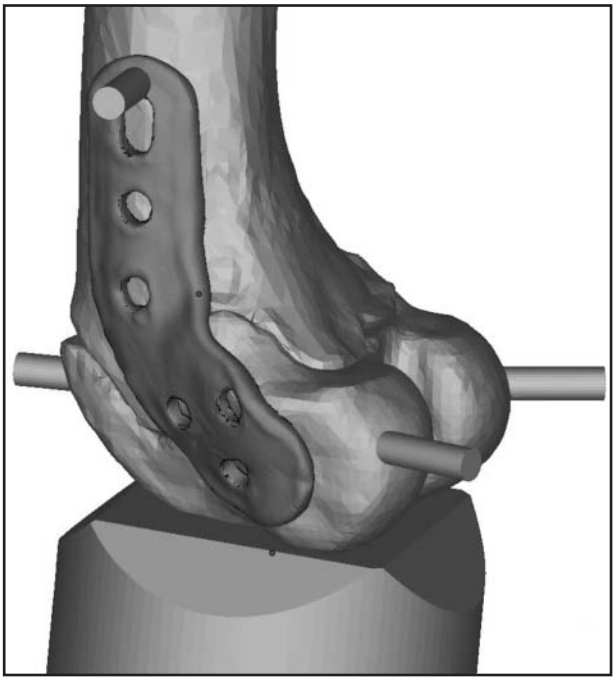

Figure 2—Illustration of a custom bone plate on the bone surface of a 3-D rendering of the lateral aspect of the proximal and distal portions of a model of a skeletally immature canine femur. The plate matches the contour of the bone. A 2-mm-thick bioresorbable PCL plate and a titanium plate were fabricated on the basis of that design.

tion molds of the 2- and 4-mm-thick plates (**Figure 3**). The molds were constructed of resin[k] by use of stereolithographic free-form fabrication[l] (**Figure 4**) and were reinforced by use of liquid steel epoxy.[m]

Polycaprolactone beads[n] were warmed to 30°C for 10 minutes, then used for injection molding at 150°C and 2.76 MPa. The surfaces and holes of the medial and lateral TNP and TKP were finished by use of a drill press rotating at 620 rotations/min.

Metal implants design and fabrication—The shape of the CTP was identical to the lateral TNP. The CAD files of the lateral TNP were imported into an electron-beam melting machine with a build platform measuring 210 × 210 × 10 mm by use of CAD software.[e] The CTP was built in titanium alloy via electron-beam melting free-form fabrication.[o] The surfaces of the CTP were finished by use of a handheld drill and the drill press.

Commercial stainless steel plates made for the repair of fractures of the distal portion of the left femur were used.[p] The CSP was shortened to 7 holes with an aluminum oxide wheel on a water-cooled abrasive cutoff saw.[q] Dimensions of the TNP, TKP, CTP, and CSP were measured with a pair of calipers.

Surgical placement of implants—A randomized block design was used to determine the order of surgery and mechanical testing. Surgeries included the placement of 2 medial and 2 lateral Kirschner wires[r] (**Figure 5**), a medial and lateral TNP (**Figure 6**), a medial and lateral TKP (**Figure 7**), a lateral CTP (**Figure 8**), and a lateral CSP (**Figure 9**). New 3.5-mm cortical bone screws were used for the fixation of all plates.[r] The screws used for the CSP were made of 316L stainless steel, and the screws used for the TNP, TKP, and CTP were made of titanium. The duration of all surgical procedures was recorded.

Mechanical testing—The screws were tightened before testing to 1.13 Nm for the CTP and CSP and 0.283 Nm for the TNP and TKP by use of a calibrated torque wrench.[s] The constructs were tested nondestructively in caudal bending, lateral bending, and internal rotation (torsion) by use of a materials testing machine with a servo-hydraulic axial torsion frame.[t] The testing parameters were selected during preliminary testing of additional replicas.

For nondestructive testing, the first load was used for preconditioning and data were recorded during the 3 subsequent loads. Caudal cantilever bending was applied by clamping the cylindrical base of the bone model, holding the construct horizontally with its cranial aspect oriented upward, and displacing the crosshead downward at a rate of 0.5 mm/s so that it placed a force of 10 N applied 100 mm proximal to the fracture repair site. Lateral cantilever bending was applied by clamping the cy-

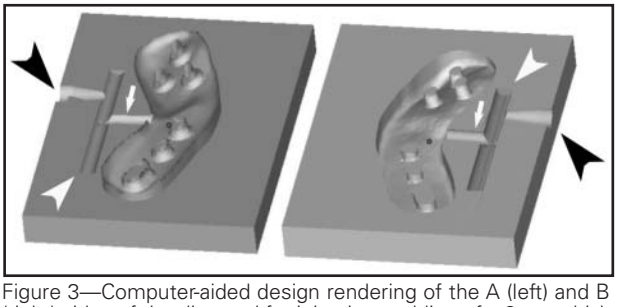

Figure 3—Computer-aided design rendering of the A (left) and B (right) sides of the die used for injection molding of a 2-mm-thick bioresorbable PCL plate. The sprue (black arrowheads), runner (white arrowheads), and gate (white arrows) are visible.

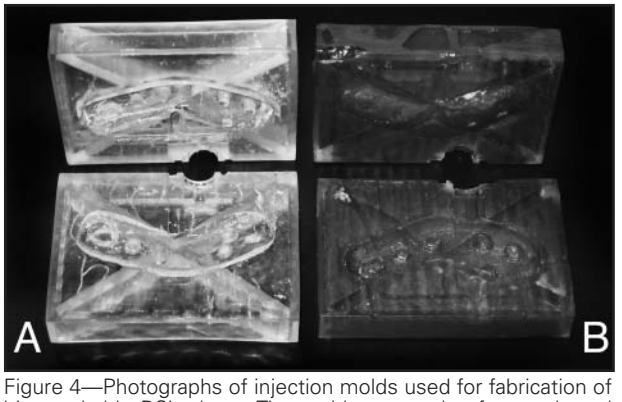

Figure 4—Photographs of injection molds used for fabrication of bioresorbable PCL plates. The molds are made of epoxy-based photopolymer fabricated by use of stereolithography (A) and reinforced with liquid steel epoxy (B).

Figure 5—Photograph of the cranial (left) and lateral (right) aspects of a canine femoral replica stabilized by use of four 2-mm-diameter stainless steel Kirschner wires. The wires were placed in a distal to proximal direction and protrude through the near and far cortices.

Figure 6—Photograph of the cranial (left) and lateral (right) aspects of a canine femoral replica stabilized by use of two 2-mm-thick PCL bioresorbable plates. Each plate is secured with six 3.5-mm titanium cortical bone screws.

Figure 7—Photograph of the cranial (left) and lateral (right) aspects of a canine femoral replica stabilized by use of two 4-mm-thick PCL bioresorbable plates. Each plate is secured with 6 titanium 3.5-mm cortical bone screws.

lindrical base of the bone model, holding the construct horizontally with its medial aspect oriented upward, and displacing the crosshead downward at a rate of 0.5 mm/s so that it placed a force of 10 N applied 100 mm proximal to the fracture repair site. Torsion was applied by clamping the cylindrical base of the bone model to the base plate, holding the construct vertically, placing a 9.8-mm-diameter metal rod in the hole in the proximal portion of the femoral shaft model, removing the slack in the system, and externally rotating the proximal portion of the femur by 2° at a rate of 10°/min. This corresponded to 2° of internal torsion (of the distal portion of the femur in relation to the femoral shaft). Construct craniocaudal stiffness, mediolateral stiffness, torsional stiffness, and deformation under load were calculated.

Within each group, constructs were randomly assigned to destructive testing (load to failure) by internal torsion or caudal cantilever bending. The testing protocols and crosshead speed for destructive loading were similar to those for nondestructive loading. Load to failure and mode of failure after internal torsion and caudal cantilever bending were recorded.

Statistical analysis—Normality of data distribution was assessed with the Shapiro-Wilk test before all comparisons were made.[u] For normally distributed data, the stiffness measured during the first, second, and third nondestructive loading events was compared with 2-tailed Student *t* tests. The stiffnesses of all construct types were compared via 1-way ANOVA with a Bonferroni correction.[v] For data that were not normally distributed, comparisons among groups were made with Mann-Whitney-Wilcoxon tests. Statistical significance was set at values of $P < 0.05$ except for the Mann-Whitney-Wilcoxon tests, in which significance for comparisons of construct stiffness between groups was set at $P < 0.00625$ for nondestructive testing, $P < 0.00625$ for the duration of surgical placement of implants, and $P < 0.0125$ for destructive testing.

Results

Constructs—Mean dimensions (width × thickness in millimeters) of the lateral TNP, lateral TKP, CTP, and CSP were 18.5 × 2.2, 19.9 × 4.5, 18.4 × 2.4, and 18.6 × 4.5, respectively. The dimensions of the medial TNP and TKP were 18.3 × 2.1 and 17.9 × 4.0, respectively.

Surgical placement—Mean ± SD durations for the surgical placement of the 4KW, TNP, TKP, CTP, and CSP were 3 ± 1 minutes, 13 ± 4 minutes, 13 ± 3 minutes, 7 ± 4 minutes, and 9 ± 2 minutes, respectively. Surgical placement of 4KW was more rapid than placement of other implants ($P < 0.001$). Surgical placement of the CSP was more rapid than placement of TKP ($P < 0.002$) and TNP ($P < 0.005$) constructs.

Mechanical testing—Forty constructs were tested (8 for each of the 5 types of constructs). Data for 118 nondestructive tests were recorded. Torsional testing could not be performed for two 4KW constructs because of fracture during setup (n = 1 construct) or software difficulties (1). For caudal cantilever bending, the mean stiffness of CTP and CSP constructs was greater than that of TNP, TKP, and 4KW constructs, and the mean stiffness of TNP and TKP constructs was greater than that of 4KW constructs (**Table 1**). For lateral cantilever bending, the mean stiffness of TKP constructs was greater than that of 4KW constructs. Similar differences in construct deformation under load were identified. Significant differences in torsional stiffness among construct types were not identified (statistical power ranging from 0.54 to 0.99).

Data for 38 destructive tests were recorded (**Table 2**). One 4KW construct fractured during setup, and software difficulties occurred for 1 TNP construct. The modes of failure included a loss of reduction without signs of fracture or plastic deformation of the implants, lateral or medial femoral condylar fractures, or plastic deformation of the implants. During caudal bending, the 4KW constructs failed by fracture of the medial aspect of the femoral condyle (n = 3 constructs) or loss of reduction (1). The TNP constructs failed by plastic deformation of the implants (n = 2) or fracture of the lateral femoral condyle (1). The TKP constructs failed by loss of reduction (n = 1), femoral shaft fracture at a screw insertion site (1), or fracture of the medial (1) or lateral (1) aspect of the femoral condyle. The CSP constructs failed by loss of reduction (n = 3) or fracture of the lateral femoral condyle (1). The CTP constructs failed by loss of reduction (n = 3) or femoral shaft fracture at a screw insertion site (1).

During torsion, the 4KW constructs failed by fracture of the lateral aspect of the femoral condyle (n = 2) or the femoral shaft (1). The TNP constructs failed by femoral shaft fracture (n = 3) or plastic deformation of the implant (1). The TKP constructs failed by femoral shaft fracture (n = 3) or fracture at a screw insertion site (1). The CSP constructs failed by femoral shaft fracture (n = 3) or plastic deformation of the bone replica (1). The CTP constructs failed by femoral shaft fracture (n = 4). Even though the yield strength and torque were numerically higher for CTP constructs than for other constructs, significant differences in yield strength and torque were not found among construct types (statistical power ranging from 0.85 to 0.99 for yield strength and 0.45 to 0.97 for yield torque). Significant differences in ultimate strength and torque were also not identified (statistical power ranging from 0.45 to 0.97 for ultimate strength and 0.67 to 0.99 for ultimate torque).

Figure 8—Photograph of the cranial (left) and lateral (right) aspects of a canine femoral replica stabilized by use of a CTP and 6 titanium 3.5-mm cortical bone screws.

Figure 9—Photograph of the cranial (left) and lateral (right) aspects of a canine femoral replica stabilized by use of a CSP and 7 stainless steel 3.5-mm cortical bone screws. The plate has been contoured to approximate the surface of the bone and has been cut at its proximal aspect.

Table 1—Mean ± SD stiffness and displacement data for 5 types of constructs (8 tests/construct type).

Construct	Caudal cantilever bending stiffness (kN/m)	Deformation during caudal cantilever bending (mm)	Lateral cantilever bending stiffness (kN/m)	Deformation during lateral cantilever bending (mm)	Torsional stiffness (internal rotation; Nm/rad)	Displacement during torsional testing (mm)
4KW	4.7 ± 1.5[a]	2.22 ± 1.50[a]	18.4 ± 7.5[a]	0.76 ± 0.30[a]	54.3 ± 8.2[a]	1.76 ± 0.23[a]
TNP	12.9 ± 3.2[b]	0.86 ± 0.23[b]	25.9 ± 4.2[a,b]	0.43 ± 0.06[a,b]	67.9 ± 9.7[a]	2.12 ± 0.51[a]
TKP	14.4 ± 3.7[b]	0.79 ± 0.20[b]	31.5 ± 4.7[b]	0.37 ± 0.06[b]	63.2 ± 13.3[a]	2.11 ± 0.43[a]
CTP	24.1 ± 4.7[c]	0.46 ± 0.09[c]	24.8 ± 7.5[a,b]	0.48 ± 0.13[a,b]	66.0 ± 14.8[a]	2.24 ± 0.46[a]
CSP	24.7 ± 4.7[c]	0.46 ± 011[c]	24.7 ± 4.5[a,b]	0.46 ± 0.07[a,b]	60.9 ± 7.8[a]	1.93 ± 0.29[a]

[a–c]Values with different superscript letters within a column indicate significant ($P < 0.05$, except for caudal and lateral cantilever bending and torsional testing [$P < 0.00625$]) differences among types of constructs.
The constructs were replicas of a canine femur and were stabilized by use of 5 stabilization methods.

Table 2—Mean ± SD loads to yield and failure for 5 types of constructs (4 tests/construct type).

Construct	Caudal cantilever bending yield strength (N)	Caudal cantilever bending ultimate strength (N)	Yield torque (Nm)	Ultimate torque (Nm)
4KW	15.1 ± 3.1[a]	92.2 ± 15.3[a]	3.3 ± 1.8[a]	11.5 ± 1.5[a]
TNP	15.6 ± 10.5[a]	108.3 ± 11.6[a]	2.8 ± 0.4[a]	8.8 ± 1.6[a]
TKP	16.2 ± 10.8[a]	83.0 ± 4.2[a]	3.5 ± 0.8[a]	8.6 ± 0.8[a]
CTP	29.5 ± 19.7[a]	82.4 ± 17.1[a]	5.1 ± 2.7[a]	8.6 ± 2.9[a]
CSP	13.6 ± 6.4[a]	65.1 ± 18.6[a]	2.3 ± 1.3[a]	8.2 ± 2.4[a]

[a,b]Values with different superscript letters within a column indicate significant differences ($P < 0.05$, except for caudal and lateral cantilever bending and torsional testing [$P < 0.0125$]) among types of constructs.
The constructs were replicas of a canine femur and were stabilized by use of 5 stabilization methods.

Discussion

Physeal fractures of the distal portion of the femur are among the most common physeal fractures in dogs.[8] Their repair is challenging because of the small size of epiphyseal fragments, the proximity of articular cartilage, the relative softness of immature bone, and the need to avoid premature closure. Salter-Harris type III and IV fractures of the distal femoral physis may be successfully managed with bone screws placed across the metaphysis or epiphysis.[9,10] Salter-Harris type I and II fractures, however, require fixation with Kirschner wires[1] or a bone plate placed across the physis.

We designed a biodegradable plate as an early developmental step toward the fabrication of resorbable implants that could stabilize Salter-Harris type I fractures. Several aspects of these free-form bioresorbable plates should be further evaluated before these plates are considered for clinical use. The increased dissection required to place 2 plates would possibly increase the likelihood of complications involving musculoskeletal soft tissues, including loss of range of motion in the stifle joint due to periarticular fibrosis or contracture of the quadriceps femoris muscle. The increased periosteal stripping and increased contact area between the bioresorbable plates and the femur could negatively impact fracture healing. Periosteal stripping has been shown to lead to a 20% decrease in cortical blood flow in an ovine tibia model.[11] Furthermore, large contact area between a bone plate and the bone surface has been postulated to induce osteoporosis[12]; however, limited dynamic compression plates and limited contact plates did not appear advantageous over conventional plates when stabilizing fractured tibiae of skeletally immature sheep.[13] Bioresorbable plates could limit bone growth. Resorbable plates do not appear to interfere with bone skull growth in childen.[5,14] However, long bones in dogs grow more rapidly than human skulls, and the impact of bioresorbable plates on the growth of long bones in dogs has not been evaluated, to our knowledge.

The availability of free-form bioresorbable plates is limited. Their design and fabrication require implant design software and equipment for free-form fabrication and injection molding. The cost of design and fabrication of the first pair of thin or thick bioresorbable plates and 12 screws used in the present study was 19 times as high as the cost of the 4KW and was 2.3 times as high as the cost of the commercial bone plate and 7 screws used. This high cost could be considered acceptable if a custom implant were needed for the management of a complex medical situation. The cost of PCL material, however, represented only 0.8% and 1.6% of the overall cost of design and fabrication of the thin and thick PCL plates, respectively. The cost of fabrication of each of the 7 additional pairs of thick bioresorbable plates and 12 screws was only 4.3 times as high as the cost of the 4KW and was half of the cost of the commercial plate and 7 screws. Custom bioresorbable implants fabricated in larger numbers for semicustom applications would have a low cost.

We used free-form fabrication to make the implants because it allowed us to optimize implant geometry and to increase implant-bone contact, which increased the stability of our constructs. Free-form biodegradable implants have not been used for fracture repair, to our knowledge. Other fracture repair groups included a commercial metal plate, a free-form custom metal plate, and Kirschner wires. We optimized the mechanical properties of constructs prepared using Kirschner wires by selecting wires with a relatively large diameter

(2 mm), placing 2 wires from each side of the bones, and penetrating the femoral shaft with the proximal end of the wires. Crossed wire constructs were stronger than other wire constructs in an ex vivo study[15] of fractures of the distal portion of the femur in dogs. All screws used in our project were made of metal. Biodegradable screws were not used because of their lower stiffness than metal screws and may have decreased our ability to detect differences between results for the bone plates. Bioresorbable plates are most often secured by use of resorbable screws[16] but are sometimes secured with metal screws.[6,17]

The 4KW stabilization method was the fastest method used in the present study. The CTP was numerically, but not significantly, the fastest plating method, most likely because plate contouring was not necessary with the CTP and because the CTP had 6 screws, whereas the CSP had 7. This observation was similar to findings when a corrective osteotomy of the proximal portion of the tibia was stabilized by use of commercial or custom plates in another study.[7] Placement of TNP and TKP was slower than that for the metal plates because 2 biodegradable plates were placed on the bone rather than 1 metal plate. Our nondestructive testing protocol included caudal and lateral cantilever bending and internal rotation of the extremity in relation to the proximal portion of the femur. The bending and torsion directions were selected on the basis of the anticipated physiologic bending forces and moments present in the femur during locomotion.[18] Destructive testing was limited to caudal cantilever bending and torsion because we anticipated that the constructs would be weakest when tested in these directions.

By being equal or superior to the properties of 4KW constructs, the mechanical properties of TNP and TKP constructs were clinically acceptable. Biodegradable plates were deemed clinically appropriate for the repair of mandibular fractures in a finite element analysis study.[19] Differences between the mechanical properties of TNP and TKP were not identified in the study reported here. This is probably because the impact of the low bending stiffness of the PCL plates was minimized by the facts that plates were placed on the medial and lateral aspect of the bone and that construct stability was the result of the proximity and fit of the proximal and distal fragments. Fragment interdigitation is reportedly a key factor in the stability of repaired Salter-Harris fracture of the distal portion of the femur in dogs.[15] Fragment interdigitation was subjectively lowest in caudal cantilever bending. The biodegradable plate constructs were stiffer than the 4KW constructs when tested in that direction, but as anticipated, they were less stiff than the metal plate constructs.

The absence of detectable differences in yield and ultimate loads to failure suggested that the bone replicas were the weakest part of the constructs. The variation in modes of failure (ie, medial or lateral femoral condylar fractures, femoral shaft fractures, and plastic deformation of the TNP) indicated that the models did not have a specific weakness and that their mechanical behavior approximated the behavior of skeletally immature canine bones. This relative weakness limited our ability to detect differences in mechanical properties between the 2 biodegradable plate constructs and between the 2 metal plate constructs. The replicas could have been made stronger by eliminating their foam cores, but the intent of the study was to create clinically realistic replicas with thin cortices and large cancellous bone areas, such as those found in skeletally immature bones.

Clinical use of free-form fabrication biodegradable plates would require optimization of the rate of decrease in strength and stiffness of the plates. In an experimental model of skull growth, plates with slow resorption rates negatively impacted bone growth.[20] Polycaprolactone was selected for the project reported here because of its availability, known biocompatibility, resorption rate, and physical and biomechanical properties.[21,22] Unlike other polymers that undergo rapid bulk degradation in vivo, PCL degrades through nonenzymatic ester hydrolysis.[21,23] It can also maintain its mechanical properties for several months in vivo.[21] The resorption rate of PCL polymers may be accelerated by pretreatment with sodium hydroxide or lipase[24] or may be slowed by blending PCL with other compounds such as 20% weight tricalcium phosphate or phosphate glass fibers.[24,25] Its mechanical properties may be enhanced with the addition of hydroxyapatite.[26] Plate resorption rates do not appear to be influenced by the presence of cyclic loading.[27]

Few reports exist of free-form fabrication of biodegradable polymer implants. The most common polymers used in fracture repair are poly-L-lactic acid, polyglycolic acid, and polydioxanone. Polycaprolactone has a lower modulus of elasticity (0.34 GPa) than do poly-L-lactic acid (2.4 to 10 GPa), polyglycolic acid (6.5 GPa), and polydioxanone (3 to 5 GPa).[28,29] However, the tensile strength of PCL (20 to 41 MPa) is comparable to that of poly-L-lactic acid (11.4 to 72 MPa), polyglycolic acid (57 MPa), and polydioxanone (56 MPa).[28,30] The low melting temperature of PCL (60°C) facilitated preparation of custom plates through injection molding. Polylactic acid may also be used in injection molding, but its high melting temperature (173°C) would require the use of molds made of high-temperature epoxy-based resins (ie, an epoxy-based resin containing ceramic nanoparticles) rather than the general epoxy-based resin used in the study reported here. The cost of a high-temperature epoxy-based resin is approximately 30% higher than the cost of a general epoxy-based resin. Shear control injection molding has been used to produce polylactic acid and PCL implants with enhanced mechanical properties.[31] Biodegradable polylactic acid implants have been produced through 3-D printing,[32] another free-form fabrication method, but their clinical use has not been reported to our knowledge.

Whereas the process for the production of free-form biodegradable implants described in the present report involves many design and fabrication steps that would make it too cumbersome and costly for specific patients, their production by use of injection molding is technically simple and affordable. Biodegradable implants could be produced through the methods described here in multiple sizes, fitting the metaphyseal and epiphyseal regions of long bones of skeletally immature dogs that could be available for the management of specific physeal fractures. Because the anatomy of metaphyseal and epiphyseal re-

gions of long bones is fairly consistent, individually customized implants would probably be unnecessary. The safety and efficacy of free-form biodegradable implants could be evaluated in a clinical trial.

In the study reported here, the mechanical properties of constructs made by use of free-form fabricated PCL biodegradable plates compared favorably with constructs made by use of Kirschner wires. Constructs made by use of metal plates compared favorably with other constructs in regard to caudal bending stiffness. The impact of PCL plates on musculoskeletal soft tissues, bone healing, and bone growth should be evaluated before free-form PCL biodegradable plates are clinically used for fracture stabilization of skeletally immature bones.

a. Siemens SOMATOM Sensation 16-slice configuration, Siemens Medical Solutions Inc, Malvern, Pa.
b. Mimics, version 8.11, Materialize USA LLC, Ann Arbor, Mich.
c. ClayTools, version 1.2, SensAble Technologies Inc, Woburn, Mass.
d. PHANTOM Omni haptic device, SensAble Technologies Inc, Woburn, Mass.
e. Magics, version 12.0.1, Materialis USA LLC, Leuven, Belgium.
f. Dimension FDM, Stratasys Inc, Eden Prairie, Minn.
g. Mold Max 30, Smooth-On Inc, Easton, Pa.
h. BJB TC-300 foam, Burman Industries, Van Nuys, Calif.
i. Bone meal, Scotts Miracle-Gro Co, Marysville, Ohio.
j. EP5340 resin, Eager Polymers Co, Chicago, Ill.
k. Somos 11110 WaterShed resin, DSM Somos, Elgin, Ill.
l. SLA-190 stereolithography machine, 3D Systems, Rock Hill, SC.
m. Loctite Fixmaster, Fel-Pro Chemical Products, Commerce City, Colo.
n. Tone Polymer P-787, Union Carbide Corp, Houston, Tex.
o. Arcam A2, Arcam AB, Mölndal, Sweden.
p. J-428U 3.5-mm distal femoral plate, Jorgensen Laboratories Inc, Loveland, Colo.
q. CD600, Mark V Laboratory Inc, East Granby, Conn.
r. Synthes Ltd, West Chester, Pa.
s. DSD-4 torque screwdriver, Imada Inc, Northbrook, Ill.
t. MTS 858 Mini Bionix II, MTS System Corp, Eden Prairie, Minn.
u. Excel Toolkit, PRA Center, Syracuse Research Corp, Syracuse, NY.
v. Excel Analysis ToolPak, Microsoft Corp, Redmond, Wash.

References

1. Whitney WO, Schrader SC. Dynamic intramedullary crosspinning technique for repair of distal femoral fractures in dogs and cats: 71 cases (1981–1985). *J Am Vet Med Assoc* 1987;191:1133–1138.
2. Edgard-Rosa G, Launay F, Glard Y, et al. Salter and Harris type-II distal femoral physeal fracture-separations at adolescent age: a new therapeutic approach (preliminary study) [in French]. *Rev Chir Orthop Réparatrice Appar Mot* 2008;94:546–551.
3. Stone EA, Betts CW, Rowland GN. Effect of Rush pins on the distal femoral growth plate of young dogs. *Am J Vet Res* 1981;42:261–265.
4. Mazzonetto R, Paza AO, Spagnoli DB. A retrospective evaluation of rigid fixation in orthognathic surgery using a biodegradable self-reinforced (70L:30DL) polylactide. *Int J Oral Maxillofac Surg* 2004;33:664–669.
5. Eppley BL, Morales L, Wood R, et al. Resorbable PLLA-PGA plate and screw fixation in pediatric craniofacial surgery: clinical experience in 1883 patients. *Plast Reconstr Surg* 2004;114:850–856.
6. Saikku-Bäckström A, Räihä JE, Välimaa T, et al. Repair of radial fractures in toy breed dogs with self-reinforced biodegradable bone plates, metal screws, and light-weight external coaptation. *Vet Surg* 2005;34:11–17.
7. Marcellin-Little DJ, Harrysson OL, Cansizoglu O. In vitro evaluation of a custom cutting jig and custom plate for canine tibial plateau leveling. *Am J Vet Res* 2008;69:961–966.
8. Marretta SM, Schrader SC. Physeal injuries in the dog: a review of 135 cases. *J Am Vet Med Assoc* 1983;182:708–710.
9. Gomes LS, Volpon JB. Experimental physeal fracture-separations treated with rigid internal fixation. *J Bone Joint Surg Am* 1993;75:1756–1764.
10. Hara Y, Tagawa M, Ejima H, et al. Application of oriented poly-L-lactide screws for experimental Salter-Harris type 4 fracture in distal femoral condyle of the dog. *J Vet Med Sci* 1994;56:817–822.
11. Kowalski MJ, Schemitsch EH, Kregor PJ, et al. Effect of periosteal stripping on cortical bone perfusion: a laser doppler study in sheep. *Calcif Tissue Int* 1996;59:24–26.
12. Perren SM, Cordey J, Rahn BA, et al. Early temporary porosis of bone induced by internal fixation implants. A reaction to necrosis, not to stress protection? *Clin Orthop Relat Res* 1988;(232):139–151.
13. Kregor PJ, Senft D, Parvin D, et al. Cortical bone perfusion in plated fractured sheep tibiae. *J Orthop Res* 1995;13:715–724.
14. Greenberg BM, Schneider SJ. Trigonocephaly: surgical considerations and long term evaluation. *J Craniofac Surg* 2006;17:528–535.
15. Sukhiani HR, Holmberg DL. Ex vivo biomechanical comparison of pin fixation techniques for canine distal femoral physeal fractures. *Vet Surg* 1997;26:398–407.
16. Peltoniemi H, Ashammakhi N, Kontio R, et al. The use of bioabsorbable osteofixation devices in craniomaxillofacial surgery. *Oral Surg Oral Med Oral Pathol Oral Radiol Endod* 2002;94:5–14.
17. Buijs GJ, van der Houwen EB, Stegenga B, et al. Torsion strength of biodegradable and titanium screws: a comparison. *J Oral Maxillofac Surg* 2007;65:2142–2147.
18. Edwards WB, Gillette JC, Thomas JM, et al. Internal femoral forces and moments during running: implications for stress fracture development. *Clin Biomech (Bristol, Avon)* 2008;23:1269–1278.
19. Cox T, Kohn MW, Impelluso T. Computerized analysis of resorbable polymer plates and screws for the rigid fixation of mandibular angle fractures. *J Oral Maxillofac Surg* 2003;61:481–487.
20. Eppley BL, Sadove AM. Effects of resorbable fixation on craniofacial skeletal growth: a pilot experimental study. *J Craniofac Surg* 1992;3:190–196.
21. Lam CX, Hutmacher DW, Schantz JT, et al. Evaluation of polycaprolactone scaffold degradation for 6 months in vitro and in vivo. *J Biomed Mater Res A* 2009;90:906–919.
22. Sun H, Mei L, Song C, et al. The in vivo degradation, absorption and excretion of PCL-based implant. *Biomaterials* 2006;27:1735–1740.
23. Yeo A, Rai B, Sju E, et al. The degradation profile of novel, bioresorbable PCL-TCP scaffolds: an in vitro and in vivo study. *J Biomed Mater Res A* 2008;84:208–218.
24. Yeo A, Sju E, Rai B, et al. Customizing the degradation and load-bearing profile of 3D polycaprolactone-tricalcium phosphate scaffolds under enzymatic and hydrolytic conditions. *J Biomed Mater Res B Appl Biomater* 2008;87:562–569.
25. Lowry KJ, Hamson KR, Bear L, et al. Polycaprolactone/glass bioabsorbable implant in a rabbit humerus fracture model. *J Biomed Mater Res* 1997;36:536–541.
26. Guarino V, Causa F, Netti PA, et al. The role of hydroxyapatite as solid signal on performance of PCL porous scaffolds for bone tissue regeneration. *J Biomed Mater Res B Appl Biomater* 2008;86B:548–557.
27. Väänänen P, Koistinen A, Nurmi J, et al. Biomechanical in vitro evaluation of the effect of cyclic loading on the postoperative fixation stability and degradation of a biodegradable ankle plate. *J Orthop Res* 2008;26:1485–1488.
28. Daniels AU, Chang MK, Andriano KP. Mechanical properties of biodegradable polymers and composites proposed for internal fixation of bone. *J Appl Biomater* 1990;1:57–78.
29. Liptak JM, Edwards MR, James SP, et al. Biomechanical characteristics of allogeneic cortical bone pins designed for fracture fixation. *Vet Comp Orthop Traumatol* 2008;21:140–146.
30. Koleske JV. Poly(ε-caprolactone) overview. In: Salamone JC, ed. *Polymeric materials encyclopedia*. Boca Raton, Fla: CRC Press, 1996;5684–5688.
31. Altpeter H, Bevis MJ, Grijpma DW, et al. Non-conventional injection molding of poly(lactide) and poly(epsilon-caprolactone) intended for orthopedic applications. *J Mater Sci Mater Med* 2004;15:175–184.
32. Giordano RA, Wu BM, Borland SW, et al. Mechanical properties of dense polylactic acid structures fabricated by three dimensional printing. *J Biomater Sci Polym Ed* 1996;8:63–75.